Dalton Transactions

Accepted Manuscript

ROYAL SOCIETY OF CHEMISTRY

www.rsc.org/dalton

Graphical Abstract

Palladium(II) complexes of a highly basic imidazolin-2-imines and their reactivity toward smallbio-molecules

Jovana Bogojeski,[a] Jeroen Volbeda,[b]Matthias Freytag,[b]Matthias Tamm[b*]and Živadin D. Bugarčić,[a*]

The Pd(II) complexes with chelating imidazolin-2-imine ligands were synthesized, the pKa values and reactivity of these complexes were investigated.

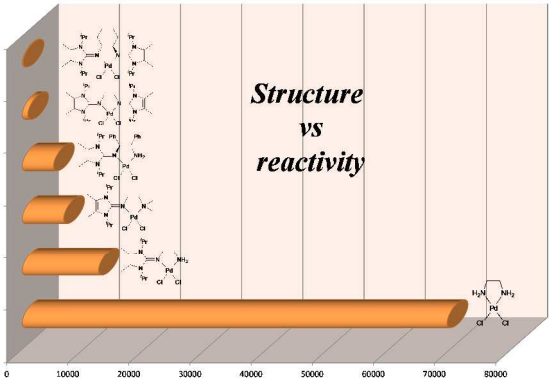

Palladium(II) complexes of highly basic imidazolin-2-imines and their reactivity toward small bio-molecules

Jovana Bogojeski,[a] Jeroen Volbeda,[b] Matthias Freytag,[b] Matthias Tamm,[b*]

Živadin D. Bugarčić[a*]

[a] *Department of Chemistry, Faculty of Science, University of Kragujevac, R. Domanovića 12, P. O. Box 60, 34000 Kragujevac, Serbia*

[b]*Institut für Anorganische und Analytische Chemie, Technische Universität Braunschweig, Hagenring 30, 38106 Braunschweig, Germany*

Corresponding authors: Prof. Dr. Živadin D. Bugarčić
Tel: +381(0)34300262
Fax: +381(0)34335040
e-mail: bugarcic@kg.ac.rs

and Prof. Dr. Matthias Tamm
Tel:+49-531-391-5309
Fax: +49-531-391-5387
e-mail: m.tamm@tu-bs.de

Abstract

A series of novel Pd(II) complexes with chelating mono(imidazolin-2-imine) and bis(imidazolin-2-imine) ligands were synthesized. The crystal structures of [Pd(DMEAIm$^{i\mathrm{Pr}}$)Cl$_2$] and [Pd(DPENIm$^{i\mathrm{Pr}}$)Cl$_2$] were determined by X-ray diffraction analysis. The reactivity of the six Pd(II) complexes, namely, [Pd(en)Cl$_2$], [Pd(EAIm$^{i\mathrm{Pr}}$)Cl$_2$], [Pd(DMEAIm$^{i\mathrm{Pr}}$)Cl$_2$], [Pd(DPENIm$^{i\mathrm{Pr}}$)Cl$_2$], [Pd(BL$^{i\mathrm{Pr}}$)Cl$_2$] and [Pd(DACH(Im$^{i\mathrm{Pr}}$)$_2$)Cl$_2$] were investigated. Spectrophotometric acid−base titrations were performed to determine the p*K*a values of the coordinated water molecules in the [Pd(en)(H$_2$O)$_2$]$^{2+}$, [Pd(EAIm$^{i\mathrm{Pr}}$)(H$_2$O)$_2$]$^{2+}$, [Pd(DMEAIm$^{i\mathrm{Pr}}$)(H$_2$O)$_2$]$^{2+}$, [Pd(DPENIm$^{i\mathrm{Pr}}$)(H$_2$O)$_2$]$^{2+}$, [Pd(BL$^{i\mathrm{Pr}}$)(H$_2$O)$_2$]$^{2+}$ and [Pd(DACH(Im$^{i\mathrm{Pr}}$)$_2$)(H$_2$O)$_2$]$^{2+}$. The substitution of the chloride ligands in these complexes by TU, L-Met, L-His and Gly was studied under *pseudo*-first-order conditions as a function of nucleophile concentration and temperature using stopped-flow techniques; the sulfur-donor nucleophiles have shown better reactivity than nitrogen-donor nucleophiles. The obtained results indicate that there is a clear correlation between the nature of the imidazolin-2-imine ligands and the acid-base characteristics and reactivity of the resulting Pd(II) complexes; the order of reactivity of the investigated Pd(II) complexes is: [Pd(en)Cl$_2$] > [Pd(EAIm$^{i\mathrm{Pr}}$)Cl$_2$] > [Pd(DMEAIm$^{i\mathrm{Pr}}$)Cl$_2$] > [Pd(DPENIm$^{i\mathrm{Pr}}$)Cl$_2$] > [Pd(BL$^{i\mathrm{Pr}}$)Cl$_2$] > [Pd(DACH(Im$^{i\mathrm{Pr}}$)$_2$)Cl$_2$]. The solubility measurements revealed good solubility of the studied imidazolin-2-imine complexes in water, despite the fact that these Pd(II) complexes are neutral complexes. Based on the performed studies, three unusual features of the novel imidazolin-2-imine Pd(II) complexes are observed, that is: good solubility in water, very low reactivity and high p*K*a values. The coordination geometries around the palladium atoms are distorted square-planar; the [Pd(DMEAIm$^{i\mathrm{Pr}}$)Cl$_2$] complex displays Pd-N distances of 2.013(2) and 2.076(2) Å, while the [Pd(DPENIm$^{i\mathrm{Pr}}$)Cl$_2$] complex displays similar Pd-N distances of 2.034(4) and 2.038(3) Å. The studied systems are of interest because little is known about the substitution behavior of imidazolin-2-imine Pd(II) complexes with bio-molecules under physiological conditions.

***Keywords*:** Palladium(II), Complexes, Kinetics, Mechanism, Reactivity

Abbreviations

en = ethylendiamine

EAIm$^{i\text{Pr}}$ = 2-(1,3-diisopropyl-4,5-dimethylimidazolin-2-imine)ethan-1-amine

BL$^{i\text{Pr}}$ = 1,2-bis(1,3diisopropyl-4,5-dimethylimidazolin-2-imino)ethane

DMEAIm$^{i\text{Pr}}$ = 2-(1,3-diisopropyl-4,5-dimethylimidazolin-2-imine)ethan-1-dimethylamine

DPENIm$^{i\text{Pr}}$ = 2-((1,3-diisopropyl-4,5-dimethylimidazolin-2-imine)-1,2-diphenylethan-1-amine

DACH(Im$^{i\text{Pr}}$)$_2$ = N,N'-(cyclohexane-1,2-diyl)bis(1,3-diisopropyl-4,5-dimethylimidazolin-2-imine)

TU = thiourea

L-Met = L-methionine

L-His = L-histidine

Gly = glycine

Introduction

The chemical behavior in solution of structurally analogous Pt(II) and Pd(II) complexes is very similar, which advanced the research progress in the area of the development of new Pd(II) complexes.[1] However, palladium(II) complexes react *ca.* 10^4–10^5 times faster than their platinum(II) analogues,[1] so the selectivity of such complexes in the binding of bio-molecules are limited which leads to low anti-tumor activity. The reaction rate of Pd(II) complexes can be slowed down and side reactions can be prevented by the introduction of inert sterically hindered ligands in the coordination sphere of the complex. A common practice in anticancer drug development is to modify leading structures in a way that maximizes cytotoxic potency toward cancer cells.[2-4]

Nowadays, cisplatin and its analogues are some of the most effective chemotherapeutic agents in clinical use for the treatment of different type of cancers.[2-5] However, the advantages and drawbacks of the widely used platinum-based anticancer drug cisplatin, prompted a search for analogous transition metal complexes.[3,4,6] To overcome the disadvantages of cisplatin, a huge number of metal ion complexes, among which are the Pd(II) complexes, were synthesized and tested.[7-9]

The chemistry of imidazolin-2-imine ligands draws attention because of the characteristic ability of imidazolines for effective acquisition and stabilization of a positive charge which leads to pronounced basic properties of the nitrogen donor atoms and the formation of the highly stable nitrogen-metal bonds.[10] These features make imidazolin-2-imines ideal ancillary ligands for applications in homogeneous catalysis. Over the past 10 years, this has led to the synthesis and application of a significant number of their metal complexes (from main group elements to lanthanides and actinides) in coordination chemistry and homogeneous catalysis.[10-12]

We anticipated that the great electron donating capacity and bulkiness of the mono- and bis(imidazolin-2-imine) ligands would result in Pd(II) complexes with greatly reduced reactivity; these complexes should in turn have an increased potential as anti-tumor agents. Figure 1 shows the structures of the Pd(II) complexes used in this study.

Figure 1.

Results and Discussion

Ligands synthesis

The ligands were synthesized in analogy to the procedure described in a previous publication.[13] Stirring one equivalent of 2-chloro-1,3-diisopropyl-4,5-dimethylimidazolium salt, six equivalents of KF, three equivalents of triethylamine and the appropriate amount of different amines in acetonitrile overnight at room temperature gave the desired ligand salts (Scheme 1). The deprotonation of the imidazolin-2-imine ligand salts was performed by stirring with KO^{t}Bu in THF for a couple of days at room temperature, with exception of the [DPEN(Im^{iPr}H)NH$_2$][BF$_4$] ligand salt, which was deprotonated by heating a THF solution overnight with NaNH$_2$ at 40 °C.

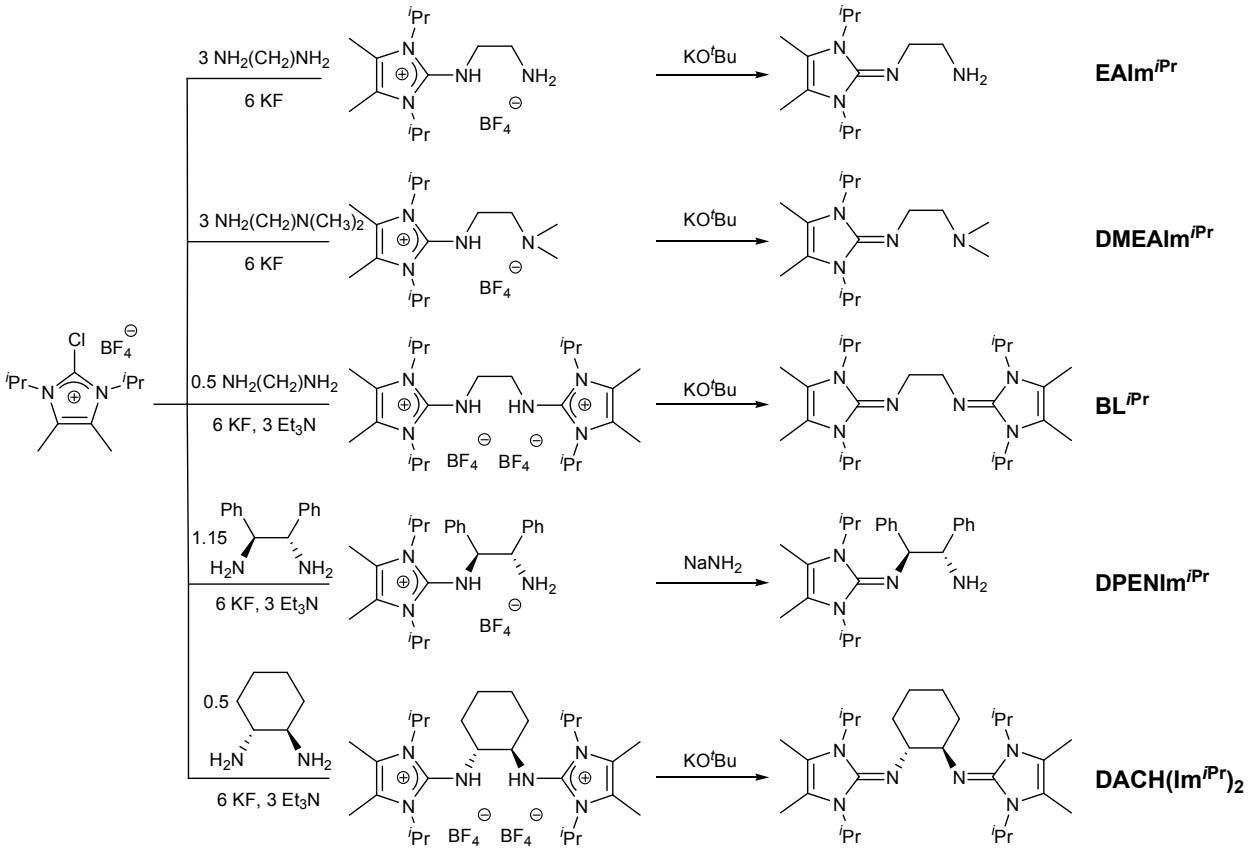

Scheme 1. Synthesis of bidentate imidazolin-2-imine ligands starting from 2-chloro-1,3-diisopropyl-4,5-dimethylimidazolium tetrafluoroborate

All imidazolin-2-imine ligands (Scheme 1), together with the corresponding dicationic tetrafluoroborate salts, were characterized by ^{1}H, ^{13}C, ^{19}F NMR, elemental analysis and ESI-MS spectroscopy. These analytical methods confirmed the formation of the imidazolin-2-imines.

Complex synthesis

The complexes shown in Figure 1 were synthesized by stirring equimolar amounts of $[Pd(COD)Cl_2]$ and the imidazolin-2-imine ligands in THF. The Pd(II) complexes $[Pd(EAIm^{iPr})Cl_2]$, $[Pd(DMEAIm^{iPr})Cl_2]$, $[Pd(DPENIm^{iPr})Cl_2]$ and $[Pd(DACH(Im^{iPr})_2)Cl_2]$ were characterized by ^{1}H and ^{13}C NMR spectroscopy, elemental analysis and ESI-MS mass spectrometry. For the complexes $[Pd(DMEAIm^{iPr})Cl_2]$ and $[Pd(DPENIm^{iPr})Cl_2]$, single crystals suitable for the X-ray analysis were also obtained.

The ^{1}H NMR as well as the ^{13}C NMR spectra of the $[Pd(EAIm^{iPr})Cl_2]$ and $[Pd(DMEAIm^{iPr})Cl_2]$ complexes display a set of signals for the imidazolin moiety, significantly shifted, compared to the free ligand. In addition, the methyl groups of the isopropyl substituents afford two doublets in the ^{1}H NMR spectrum. This indicates hindered rotation along the imine C-N bond on the NMR timescale at room temperature, which has previously been observed for related complexes, bearing both chiral and achiral ligands.[10-13] The achiral Pd(II) complex, $[Pd(BL^{iPr})Cl_2]$,[14] shows just one doublet in the ^{1}H NMR spectra for the methyl groups of the isopropyl substituents. The $[Pd(DPENIm^{iPr})Cl_2]$ and $[Pd(DACH(Im^{iPr})_2)Cl_2]$ exhibit four doublets in the ^{1}H NMR spectrum, which is expected considering that ligands $DPENIm^{iPr}$ and $DACH(Im^{iPr})_2$ show diastereotopic signals for the methyl substituents on the isopropyl groups combined with a hindered rotation around the imine C-N bond in the Pd(II) complex.

The mass spectrum of $[Pd(DACH(Im^{iPr})_2)Cl_2]$ in the *m*/*z* range of 400−700 includes main peaks at *m*/*z* = 471 (1+), 575 (2+), and 611 (1+), which correspond to $[(DACH(Im^{iPr})_2)H]^+$, $[Pd(DACH(Im^{iPr})_2)]^{2+}$ and $[Pd(DACH(Im^{iPr})_2)Cl]^+$ and represent fragments of the $[Pd(DACH(Im^{iPr})_2)Cl_2]$ complex. Furthermore, Figure S1 depicts the isotopic pattern at *m*/*z* = 611.28, which belongs to the $[Pd(DACH(Im^{iPr})_2)Cl_2]$ complex, without one chloride ion, *ie*. $[Pd(DACH(Im^{iPr})_2)Cl]^+$ and its corresponding simulated pattern.

Preparation and structure of [Pd(DMEAIm$^{i\mathrm{Pr}}$)Cl$_2$]

The reaction of DMEAIm$^{i\mathrm{Pr}}$ with [Pd(COD)Cl$_2$] (COD = 1,5-cyclooctadiene) in THF afforded the complex [Pd(DMEAIm$^{i\mathrm{Pr}}$)Cl$_2$] as a deep-red solid. Red crystals suitable for X-ray diffraction analysis were isolated from a dichloromethane/n-hexane solution, and the molecular structure of [Pd(DMEAIm$^{i\mathrm{Pr}}$)Cl$_2$] is shown in Figure 2. The molecule crystallizes in the orthorhombic space group *P*nma, with one co-crystallized molecule of CH_2Cl_2 per asymmetric unit and one is located on a crystallographic mirror plane. The ligand is coordinated to the palladium atom in a chelating, bidentate fashion with an N1-Pd-N2 bite angle of 83.08(9)°. The Pd-N bond lengths are 2.013(2) and 2.076(2) Å for Pd-N1 and Pd-N2, respectively, indicating a stronger coordination of the more basic imine nitrogen to the Pd atom. The imine bond length of 1.349(4)Å (N1-C3) is long for a C=N double bond, indicating a pronounced negative charge on the imine nitrogen. This is also confirmed by the ρ-value of 0.998; the ρ-value is defined as ρ=2a/(b + c), with (a) denoting the exo- and (b) and (c) the *endo*-cyclic bond lengths within the guanidine CN_3 moiety. Values approaching unity indicate complete charge delocalization within the CN_3 fragment.[15] The electron-donating capacity of the imidazolin-2-imine is also reflected in the different Pd-Cl bond lengths, with the Pd-Cl1 bond length (2.3390(7)Å) trans to the imine nitrogen being significantly longer than the Pd-Cl2 bond length (2.2951(7)Å) trans to the tertiary amine. These structural parameters are comparable to those observed for [Pd(BL$^{i\mathrm{Pr}}$)Cl$_2$] and the $PdCl_2$ complex of tetramethylethylendiamine.[14,16]

Figure 2.

Preparation and structure of [Pd(DPENIm$^{i\mathrm{Pr}}$)Cl$_2$]

The reaction of DPENIm$^{i\mathrm{Pr}}$ with [Pd(COD)Cl$_2$] in THF afforded the complex [Pd(DPENIm$^{i\mathrm{Pr}}$)Cl$_2$] as an orange-red solid. Red crystals suitable for X-ray diffraction analysis were isolated from an acetone/n-hexane solution, and the molecular structure of [Pd(DMEAIm$^{i\mathrm{Pr}}$)Cl$_2$] is shown in Figure 3. The compound crystallizes in the orthorhombic space group $P2_12_12_1$ with four independent complexes, five molecules of acetone and on molecule of hexane per asymmetric unit. The ligand is coordinated to the palladium atom in a chelating,

bidentate fashion with an N1-Pd-N2 bite angle of 82.69(14)°. The Pd-N bond lengths are virtually identical at 2.034(4) and 2.038(3) Å for Pd-N1 and Pd-N2, respectively. The imine C15-N1 bond length of 1.367(5)Å is long for a C=N double bond and the corresponding ρ-value of 1.004 indicates a strong negative charge on the exocyclic imine nitrogen atom. Again, the Pd-Cl2 (2.3395(10)Å) distance trans to the imine nitrogen is longer than the Pd-Cl bond which is trans to the primary amine Pd-Cl1 (2.3193(10)Å).

Figure 3.

Solubility of the imidazolin-2-imine Pd(II) complexes

Despite the fact that the prepared Pd(II) complexes are neutral, UV-Vis spectrophotometric measurements showed that they have good solubility in water (see Table 1). The solubility of the complexes is around four times greater than that observed for cisplatin and ca. twice that of oxaliplatin. This high solubility is promising for the intended application of these complexes as anti-tumor agents. To this day, cisplatin is the most widely used metal complexes based cytostatic in the world.[2-5] One of the drawbacks of cisplatin as an anti-tumor drug is its low solubility in aqueous media, therefore an increase in water solubility is an important goal for the design of any new metallo-drug. A higher water solubility can also result in a decreased toxicity of metallo-drugs, as is the case for oxaliplatin, which has less nephrotoxicity and a higher water solubility than cisplatin.[2-5] Herein, we show that the introduction of different imidazolin-2-imines affords Pd(II) complexes which are significantly more water soluble than cisplatin.

Table 1.

p*K*a Determination of the aqua Pd(II) complexes

It is well established that the low chloride concentration of approximately 4 mM in living cells causes Pt(II) and Pd(II) dichloride complexes to form diaqua complexes upon entering the cell. These diaqua complexes then bind to the DNA.[17] There is a correlation between the p*K*a values of the coordinated water molecules and the electronic structure of the complexes and accordingly the reactivity of the complexes. Therefore, the p*K*a values of the complexes in aqueous solution were determined. This was done *via* UV-vis spectrophotometric pH titration with NaOH as a base in the pH range between 2 and 12. Each p*K*a titration was performed twice and the average of both values was taken. Figure 4 (see also Figures S2-S4 of the Supporting Information) shows a plot of absorbance versus pH at specific wavelengths, which was used to determine the p*K*a values of the coordinated water molecules. The data were fitted using a nonlinear least-squares procedure, as shown in the inset in Figure 4. The overall process can be presented by Eqs (1) and (2). The data obtained for the p*K*a values are summarized in Table 2.

$$[Pd(L)(H_2O)_2]^{2+} + H_2O \overset{Ka_1}{\rightleftharpoons} [Pd(L)(OH)(H_2O)]^{+} + H_3O^{+} \qquad (1)$$

$$[Pd(L)(OH)(H_2O)]^{+} + H_2O \overset{Ka_2}{\rightleftharpoons} [Pd(L)(OH)_2] + H_3O^{+} \qquad (2)$$

L = $DMEAIm^{iPr}$, $EAIm^{iPr}$, $DPEN(Im^{iPr})NH_2$, BL^{iPr}, $DACH(Im^{iPr})_2$

Figure 4.

Table 2.

Table 2 shows that there is a significant difference between p*K*a$_1$ and p*K*a$_2$ values. The data for $[Pd(en)(H_2O)_2]^{2+}$ (p*K*a$_1$ = 5.6, p*K*a$_2$ = 7.3)[18] represent typical values for complexes containing sp^3-hybridized amines.[19] In comparison, Pd(II) complexes with imidazolin-2-imine ligands give higher p*K*a values, in agreement with the electron-rich nature of the palladium centers in these complexes, in which deprotonation of the aqua ligand and formation of a negatively charged hydroxo-ligand is disfavored. The complexes with mono(imidazolin-2-imine) ligands, $[Pd(EAIm^{iPr})(H_2O)_2]^{2+}$, $[Pd(DMEAIm^{iPr})(H_2O)_2]^{2+}$ and $[Pd(DPENIm^{iPr})(H_2O)_2]^{2+}$ have

two different types of donors, *viz.* an imidazolin-2-imine moiety and an sp^3-hybridized primary or tertiary amine ($-NR_2$) unit. In these cases, it can be assumed that the first aqua ligand to be deprotonated would be that trans to the less electron donating amine donor.

The pH in healthy human cells lies between 7.3 – 7.4.[20] As the pKa_1 values listed in Table 2 are lower than 7.3, the formation of Pd(II) monohydroxo species can be expected. Conversely, the pH in cancer cells is lower (around 6.2 to 6.9),[20] suggesting that the hydrolyzed [Pd(DPENIm$^{i\text{Pr}}$)Cl_2] and [Pd(DACH(Im$^{i\text{Pr}}$)$_2$)Cl_2] complexes will mainly exist as diaqua species while other complexes will exist as monohydroxo species. Formation of monohydroxo species and diaqua complexes is good because Pd-OH species are more substitution-inert but Pd-OH can also act as a base, deprotonating a H-N site in nucleobases and binding to the N atom, while diaqua species can readily bind to DNA.

Kinetic studies

To get an idea of the robustness of the Pd(II) complexes in living tissue, the substitution reactions of Pd(II) complexes with selected nucleophiles (Figure 5) was investigated. The change in absorbance was followed, at suitable wavelengths, as a function of time at 310 K and pH ≈ 7.2. The proposed reaction pathways for all observed substitution processes are presented in Scheme 2. The substitution reactions of all Pd(II) complexes proceed in two successive reaction steps that are both dependent on the nucleophile concentration.

The entering ligands, L-Met, L-His and Gly, are essential amino acids; therefore, the metal complex (as an antitumor active drug) on its way from the injection to the diseased tissue will encounter them. On the basis of many investigations in the field of Pt(II) and Pd(II) complexes, it is known that both ions can easily form a bond with thioethers (such as L-Met).[1,14,17] Pt–sulfur(thioether) adducts have been postulated to be a drug reservoir for platinum and may act as intermediate platinum complexes that can be transformed into Pt–DNA adducts,[17] which makes the study of substitution reactions with L-Met very important. Thiourea was selected because it is a ligand with high solubility, neutral character and good nucleophilicity. Also, thiourea combines the ligand properties of thiolates as π donors[21] and thioethers as σ donor and π acceptor[22]. Also, thiourea is used as a protective and rescue agent to prevent side effects which are caused by Pt(II) antitumor drugs.[23,24] Therefore, the investigation

of the interactions of the selected nucleophiles and Pd(II) complexes is important for the development of potential antitumor drugs.

Figure 5.

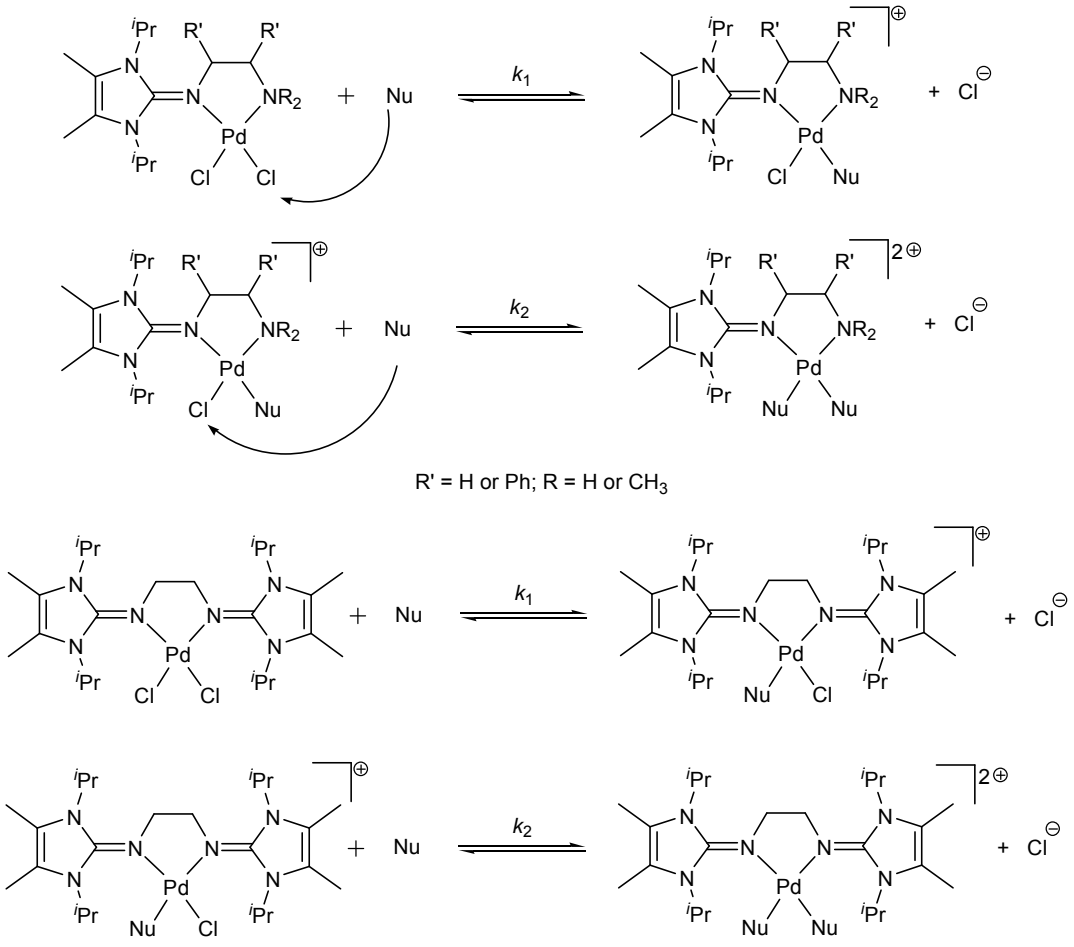

Scheme 2. Nu = TU, L-Met, L-His and Gly

The substitution reactions of square-planar metal complexes can proceed according to two parallel pathways.[25] One involves the formation of a solvent-coordinated complex, e.g. a diaqua complex, followed by rapid substitution of the coordinated solvent by the entering nucleophile (solvolytic pathway), whilst the other involves a direct nucleophilic attack by the entering nucleophile. To suppress the solvolytic pathway, a 30 mM NaCl solution was added (see Supporting Information, Figure S5). The rate constants for substitution could be determined,

under *pseudo*-first-order conditions, from a plot of the linear dependence of k_{obsd} *versus* the total nucleophile concentration, according to Eqs. (3) and (4). The slope of the line represents k_1 or k_2, whilst the intercept represents $k_{-1}[Cl^-]$ or $k_{-2}[Cl^-]$. Plots of $k_{obsd1,2}$ *versus* nucleophile concentration led to a linear dependence with no meaningful intercept for all complexes and both substitution steps. The results are summarized in Table 3 and 4.

$$k_{obsd1} = k_1[Nu] + k_{-1}[Cl^-] \approx k_1[Nu] \quad (3)$$

$$k_{obsd2} = k_2[Nu] + k_{-2}[Cl^-] \approx k_2[Nu] \quad (4)$$

Nu = TU, L-Met, Gly, L-His

Table 3.

Table 4.

As an example, the kinetic traces for [Pd(DMEAIm^{iPr})Cl$_2$] including the necessary time scales for both reaction steps are shown in Figure 6.

Figure 6.

Figure 7 shows the dependence of k_{obsd} on nucleophile concentration for the [Pd(DPENIm^{iPr})Cl$_2$] and [Pd(BL^{iPr})Cl$_2$] complexes (see also Supporting Information, Figures S6-S11).

Figure 7.

The order of reactivity of the investigated Pd(II) complexes for both reactions steps is (Table 3):

[Pd(en)Cl$_2$] > [Pd(EAIm^{iPr})Cl$_2$] > [Pd(DMEAIm^{iPr})Cl$_2$] > [Pd(DPENIm^{iPr})Cl$_2$] > [Pd(BL^{iPr})Cl$_2$] > [Pd(DACH(Im^{iPr})$_2$)Cl$_2$]

As expected, [Pd(en)Cl_2] is the most reactive of the investigated complexes, the values obtained for this complex are in line with those found for similar complexes.[1] The introduction of one imidazolin-2-imine moiety in [Pd(EAIm$^{i\text{Pr}}$)Cl_2] results in a decrease in reactivity. Compared to [Pd(en)Cl_2], the first reaction step is between five and 100 times slower. The second substitution is even more impaired and proceeds up to 1000 times slower. It appears that the strong electron donating capacity of the imidazolin-2-imine results in an electron rich Pd(II) center, which is less electrophilic and thus less susceptible to attack by bio-relevant donor molecules. [Pd(DMEAIm$^{i\text{Pr}}$)Cl_2] shows a further reduction in reactivity, the first substitution being between 10 and 100 times slower than in [Pd(en)Cl_2]. This is likely caused by an increase in electron donating and steric hindrance due to the exchange of the primary amine for a tertiary amine compared to [Pd(EAIm$^{i\text{Pr}}$)Cl_2]. [Pd(DPENIm$^{i\text{Pr}}$)Cl_2] is the least reactive of the investigated complexes bearing ligands with a single imidazolin-2-imine moiety. Its reactivity for the first substitution is reduced roughly 100 fold compared to [Pd(en)Cl_2] for all tested donor molecules. Introduction of ligands bearing two imidazolin-2-imine moieties in [Pd(BL$^{i\text{Pr}}$)Cl_2] and [Pd(DACH(Im$^{i\text{Pr}}$)$_2$)Cl_2] reduces the reactivity even further with both complexes showing a first substitution reaction that proceeds between 100 and 1000 times slower than for [Pd(en)Cl_2].

For all investigated complexes, the second substitution step is significantly slower than the first substitution. In case of the reference complex [Pd(en)Cl_2], this difference is the least pronounced. For [Pd(EAIm$^{i\text{Pr}}$)Cl_2], [Pd(DMEAIm$^{i\text{Pr}}$)Cl_2] and [Pd(DPENIm$^{i\text{Pr}}$)Cl_2], it can be assumed that the first substitution would take place next to the less sterically hindered side of the ligand *viz.* next to the amine donor. Therefore, the next substitution would have to take place next to the bulky imidazolin-2-imine donor, rendering it less facile. In addition, the first substitution would result in a less electrophilic Pd(II) center, reducing the reaction rate for the second substitution.

Interestingly, the rate constants which were obtained for the substitution reactions of the studied imidazolin-2-imine Pd(II) complexes are in line with the rate constants determined for substitution reactions of aqua Pt(II) complexes (Table S1, Suporting Imformation).[26] This confirms that the investigated complexes have decreased reactivity, since it is known that Pd(II) complexes react much faster than Pt(II) complexes.[1] The low reactivity of the investigated complexes presents the possibility that they might find biological application.

The rate constants, k_1, presented in the Table 3, indicate that the used nitrogen and sulfur donor ligands are good entering ligands in the substitution reactions with the investigated Pd(II) complexes.

The order of the reactivity of the investigated nucleophiles, for the first reaction step is: TU > L-Met > L-His > Gly, Table 3. This is the expected order of reactivity, as sulfur-donor nucleophiles react faster with Pd(II) complexes than nitrogen-donor nucleophiles. The Pd(II) ion is soft acid and will easily form bonds with a soft base such as sulfur.

The data for the second substitution step shows that TU reacts faster than L-His. Kinetic traces for reactions with L-Met and Gly gave fits with a double exponential function. The constants, k_{obsd1} and k_{obsd2}, were plotted against the concentration of the entering L-Met or Gly nucleophiles. For k_{obsd1}, a linear dependence on the nucleophile concentration was observed for all the complexes studied; k_{obsd2} was found to be independent of the L-Met or Gly concentration, suggesting a chelate formation process as presented at Scheme 3 and Figure 8.

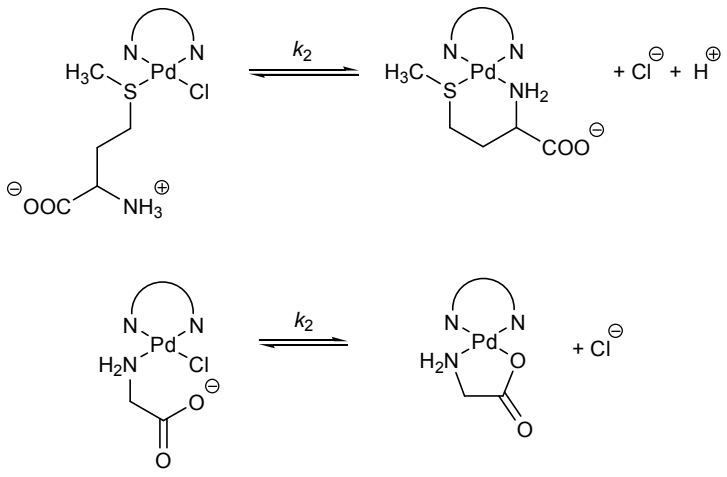

Scheme 3. The second step of the substitution reaction of investigated Pd(II) complexes with L-Met and Gly.

Figure 8.

The substitution reactions of the investigated Pd(II) complexes with L-Met proceed with a nucleophilic attack by the sulfur donor of the thioether group, and subsequently a six-

membered ring (see Scheme 3) is formed by substitution with the nitrogen donor of the amine group. The acid dissociation constants of free L-Met is: pK_{COOH} = 2.28,[27] pK_{NH3+} = 9.2[27], so ring-closure must involve deprotonation of the amine group (Scheme 3). Ring-closure and formation of a six-membered ring also occurs in the substitution reactions of Pt(II) complexes and L-Met.[17,28] In the substitution reaction between Gly and the investigated Pd(II) complexes, the formation of a five-membered ring is confirmed. The nucleophilic attack occurs *via* the nitrogen donor of the amine group and then *via* the oxygen from the carboxyl group (Scheme 3). A similar ring-closure between Pd(II) or Pt(II) complexes and Gly was observed in earlier publications.[28,29]

To confirm that the second step is chelation, the kinetics were studied with the Pd(II) complexes in excess instead of L-Met or Gly. This would mean that a two-step reaction can only occur if ring closure is involved. The obtained kinetic traces for such reactions gave fits to a double exponential function. Similar values for the rate constants were obtained, as were observed in the experiments with L-Met or Gly added in excess (see Supporting Information Figure S13 and 14). All this indicates that ring closure occurs.

Activation Parameters

The activation parameters $\Delta H^{\neq}$ and $\Delta S^{\neq}$ (Tables S2) were calculated using the Eyring equation for the reactions with TU (see Figure 9 and S12, Supporting Information) for the first and second reaction step. The activation parameters support an associative mechanism for each of these reactions which is supported by the significantly negative activation entropies. This suggests that the activation process in the studied systems is strongly dominated by bond formation.

Figure 9.

Conclusion

In conclusion, we were able to use novel imidazolin-2-imine ligands for the synthesis of a series of new Pd(II) complexes. For [Pd(DMEAIm$^{i\text{Pr}}$)Cl$_2$] and [Pd(DPENIm$^{i\text{Pr}}$)Cl$_2$], X-ray structures could be determined. Solubility measurements showed that the imidazolin-2-imine

Pd(II) complexes have good solubility in water. Spectrophotometric pH titration experiments showed two p*K*a values for the diaqua complexes of all investigated Pd(II) compounds. A clear correlation between the structure of the imidazolin-2-imine and the determined p*K*a values was found. The p*K*a values of the more electron rich complexes (*i.e*. those bearing a more electron-donating ligand) were significantly higher than those of the less electron rich complexes. Kinetic experiments were performed with selected small bio-molecules (*i.e*. thiourea, L-methionine, L-histidine and glycine) under *pseudo*-first-order conditions as a function of nucleophile concentration and temperature using stopped-flow techniques. These measurements showed that mono(imidazolin-2-imine) Pd(II) complexes react faster than bis(imidazolin-2-imine) Pd(II) complexes. This can be attributed to both electronic and steric effects of the imidazolin-2-imine ligands. Two reaction steps are observed that belong to the displacement of both chloride ligands. We found that the reactivity of the Pd(II) complexes decreases as follows: $[Pd(en)Cl_2]$ > $[Pd(EAIm^{iPr})Cl_2]$ > $[Pd(DMEAIm^{iPr})Cl_2]$ > $[Pd(DPENIm^{iPr})Cl_2]$ > $[Pd(BL^{iPr})Cl_2]$ > $[Pd(DACH(Im^{iPr})_2)Cl_2]$. The sulfur-donor ligands TU and L-Met react faster than nitrogen-donor ligands L-His and Gly. Both L-Methionine and glycine react by undergoing a ring closure as the second substitution step. The mechanism of the substitution reactions is associative supported by the negative values of $\Delta S^{\neq}$.

The coordination of imidazolin-2-imine ligands to Pd(II) gives three benefits with regard to the utilization of such complexes as metallo-drugs. The first is an increase of the solubility of these Pd(II) complexes, as the low solubility of neutral Pd(II) and Pt(II) complexes, such as cisplatin, is one of the major disadvantages in their application as cytostatics. Secondly, imidazolin-2-imine Pd(II) complexes react slower than most of the known Pd(II) complexes; their reactivity is such that it lies in the same range as that of aqua Pt(II) complexes. The reduced reactivity of Pd(II) complexes should lead to a better selectivity of such complexes in the binding of bio-molecules. Lastly, the introduction of imidazolin-2-imines leads to an increase of the p*K*a values of the coordinated water molecules in these complexes. For $[Pd(DPENIm^{iPr})Cl_2]$ and $[Pd(DACH(Im^{iPr})_2)Cl_2]$, the p*K*a values are such that it can be assumed that they will exist mostly as diaqua species at the pH of tumor cells. These combined advantages should lead to a more selective attack of these complexes at the DNA of tumor cells as a final target in drug delivery.

Acknowledgements

The authors gratefully acknowledge financial support from the Ministry of Education, Science and Technological Development Serbia, project No. 172011 and the Deutsche Forschungsgemeinschaft (DFG).

Experimental

Chemicals and solutions

Thiourea, L-methionine, L-histidine, glycine, ethylenediamine, *N,N*-dimethylethylenediamine, (1*R*,2*R*)-(-)-1,2-diaminocyclohexane, (1*S*,2*S*)-(-)-1,2-diphenylethylenediamine, $NaBF_4$, KF, $NaNH_2$, KO^tBu and $PdCl_2$ were obtained from Acros Organics or Sigma Aldrich, and were used without further purification. Hepes buffer (N-2-hydroxyethylpiperazine-N'-2-ethanesulfonic acid) was obtained from Sigma Aldrich. All the other chemicals were of the highest purity commercially available and were used without further purification. Ultra-pure water was used in all experiments. Nucleophile stock solutions were prepared shortly before use by dissolving the chemicals.

Preparation of the ligands and complexes

All reactions were performed in a glove box, under dry argon atmosphere (MBraun 200B) or on a high-vacuum line using standard Schlenk techniques, unless noted otherwise. Commercial grade solvents were purified by use of a solvent purification system from MBraun GmbH and stored over molecular sieves (4 Å) under dry argon atmosphere.

All synthesis of the ligands started from 2-chloro-1,3-diisopropyl-4,5-dimethylimidazolium tetrafluoroborate, which is prepared according to the literature procedure.[30]

Synthesis and characterization of $[DMEAIm^{iPr}H][BF_4]$ (1)

To a mixture of 10.66 g (35.2 mmol; 1 eq) of 2-Chloro-1,3-diisopropyl-4,5-dimethylimidazolium tetrafluoroborate and 12.30 g (211.2 mmol; 6 eq) KF in 90 mL of CH_3CN was added 11.5 mL (105.6 mmol; 3 eq) of *N,N*-dimethylethylenediamine. The mixture was stirred overnight at room

temperature. On air, 90 mL of $CHCl_3$ was added to the reaction mixture, which was then filtered through celite. The residue was extracted once with 20 mL of $CHCl_3$. The filtrate was washed with a dilute $NaBF_4$ solution (19.36 g (176.3 mmol) $NaBF_4$ in 100 mL water). The organic phase was separated and the aqueous phase was extracted once with 20 mL $CHCl_3$. The combined organic phases were dried over Na_2SO_4 and the solvent was then removed *in vacuo*. The product is obtained as a yellow oil (11.38 g, 32.1 mmol, 91%).

^{1}H NMR (400 MHz; $CDCl_3$): δ = 5.12 (bs, 1H, N*H*), 4.78 (sept, 2H, J_{HH} 7.0 Hz, C*H*(Me)$_2$), 3.22 (bt, 2H, J_{HH} 6.0 Hz, CNHC*H*$_2$CH$_2$), 2.59 (t, 2H, J_{HH} 6.0 Hz, CH$_2$C*H*$_2$NMe$_2$), 2.26 (s, 6H,N(C*H*$_3$)$_2$), 2.25 (s, 6H, CC*H*$_3$), 1.54 (d, 12H, J_{HH} 7.0 Hz, CH(C*H*$_3$)$_2$) ppm.

^{13}C NMR (100 MHz; $CDCl_3$): δ = 144.1 (N$_2$*C*NH), 122.9 (*C*Me), 58.7 (CH$_2$*C*H$_2$NMe$_2$), 49.9 (*C*HMe$_2$), 46.7 (CNH*C*H$_2$CH$_2$), 45.4 (N(*C*H$_3$)$_2$), 21.4 (CH(*C*H$_3$)$_2$), 10.1 (C*C*H$_3$) ppm.

^{19}F NMR (188 MHz; $CDCl_3$): δ = -152.08 (B*F*$_4$) ppm.

Anal. Calcd. for ($C_{15}H_{31}BF_4N_4$)·0.10($CHCl_3$) C: 49.53; H: 8.56; N: 15.30. Found: C: 49.43; H: 8.80; N: 15.64

ESI-HRMS: $[M\text{-}BF_4]^+$: Calcd.: 267.25487; Found: 267.25446 (Δ: 0.41 mmu).

Synthesis and characterization of [DMEAIm^{iPr}] (2) by deprotonation of (1)

To a solution of 9.00 g (25.4 mmol; 1 eq) of **1** in 220 mL of THF was added 3.42 g (30.5 mmol; 1.2 eq) KO^{t}Bu at 0 °C. The mixture was stirred and allowed to warm to room temperature, it was subsequently stirred overnight. The THF was removed *in vacuo*. The residue was extracted twice with 50 mL of pentane and filtered through celite. The solvent was removed *in vacuo*. The product was obtained as a light brown oil (6.15 g, 23.1 mmol, 91%).

^{1}H NMR (400 MHz; C_6D_6): δ = 4.43 (sept, 2H, J_{HH} 7.0 Hz, C*H*Me$_2$), 3.73 (t, 2H, J_{HH} 7.3 Hz, C=NC*H*$_2$CH$_2$), 2.66 (t, 2H, J_{HH} 7.3 Hz, CH$_2$C*H*$_2$NMe$_2$), 2.25 (s, 6H, N(C*H*$_3$)$_2$), 1.71 (s, 6H, CC*H*$_3$), 1.20 (d, 12H, J_{HH} 7.0 Hz, CH(C*H*$_3$)$_2$) ppm.

^{13}C NMR (100 MHz; C_6D_6): δ = 150.3 (N$_2$*C*=N), 115.9 (*C*Me), 64.8 (CH$_2$*C*H$_2$NMe$_2$), 49.0 (C=N*C*H$_2$CH$_2$), 46.6 (N(*C*H$_3$)$_2$), 46.3 (*C*HMe$_2$), 21.3 (CH(*C*H$_3$)$_2$), 10.9 (C*C*H$_3$) ppm.

Anal. Calcd. for ($C_{15}H_{30}N_4$) C: 67.62; H: 11.35; N: 21.03. Found: C: 67.36; H: 11.16; N: 20.67.

Synthesis and characterization of [EAIm$^{i\mathrm{Pr}}$H][BF_4] (3)

To a mixture of 1.50 g (4.95 mmol; 1 eq) of 2-Chloro-1,3-diisopropyl-4,5-dimethylimidazolium tetrafluoroborate and 1.74 g (29.9 mmol; 6 eq) of KF in 15 mL of CH_3CN was added 1.5 mL (22.2 mmol; 4,4 eq) of ethylenediamine. The mixture was stirred overnight at room temperature. After filtration, on air, through celite and subsequent washing with 20 mL of $CHCl_3$ the organic fraction was washed with a dilute $NaBF_4$ solution (2,7 g; 24.6 mmol $NaBF_4$ in 100 mL of water). The organic layer was dried over Na_2SO_4, after which the solvent was removed *in vacuo*. This gave the product as a yellow oil (1.39 g, 4.26 mmol, 86%).

^{1}H NMR (400 MHz; $CDCl_3$): δ = 4.85 (sept, 2H, J_{HH} 7.0 Hz, C*H*(Me)$_2$), 3.16 (t, 2H, J_{HH} 6.0 Hz, C=NHC*H*$_2$CH$_2$), 3.01 (t, 2H, J_{HH} 6.0 Hz, CH$_2$C*H*$_2$NH$_2$), 2.32 (bs, 2H, N*H*$_2$), 2.25 (s, 6H, CC*H*$_3$), 1.54 (d, 12H, J_{HH} 7.0 Hz, CH(C*H*$_3$)$_2$), 1.53 (bs, 2H, N*H*$_2$) ppm.

^{13}C NMR (100 MHz; $CDCl_3$): δ = 144.1 (N$_2$*C*NH), 123.0 (*C*Me), 51.4 (CNH*C*H$_2$CH$_2$), 50.0 (*C*H(Me)$_2$), 41.5 (CH$_2$*C*H$_2$NH$_2$), 21.4 (CH(*C*H$_3$)$_2$), 10.1 (C(*C*H3) ppm.

^{19}F NMR (188 MHz; $CDCl_3$): δ = -152.08 (B*F*$_4$) ppm.

Anal. Calcd. for ($C_{13}H_{27}BF_4N_4$)·0.10($CHCl_3$) C: 46.53; H: 8.08; N: 16.57. Found: C: 46.78; H: 8.03; N: 16.55.

ESI-HRMS: [M-BF_4]$^+$: Calcd.: 239.22357; Found: 239.22316 (Δ: 0.41 mmu).

Synthesis and characterization of [EAIm$^{i\mathrm{Pr}}$] (4) by deprotonation of (3)

To a solution of 1.54 g (4.7 mmol; 1 eq) of **3** in 21 mL of THF was added 0.64 g (5.7 mmol; 1.2 eq) of KO^{t}Bu. The reaction mixture was stirred for several days at room temperature. The solvent was removed *in vacuo* and the residue was extracted with three times 15 mL of pentane. The pentane was subsequently removed *in vacuo* to yield the product as an orange oil (0.87 g, 3.6 mmol, 77%).

^{1}H NMR (400 MHz; C_6D_6): δ = 4.51 (sept, 2H, J_{HH} 7.0 Hz, C*H*(Me)$_2$), 3.61 (t, 2H, J_{HH} 5.4 Hz, C=NC*H*$_2$CH$_2$), 3.01 (bt, 2H, J_{HH} 5.3 Hz, CH$_2$C*H*$_2$NH$_2$), 1.68 (s, 6H, CC*H*$_3$), 1.28 (bs, 2H, N*H*$_2$), 1.20 (d, 12H, J_{HH} 7.0 Hz, CH(C*H*$_3$)$_2$) ppm.

^{13}C NMR (100 HMz; C_6D_6): δ = 151.1 (N$_2$*C*=N), 115.8 (*C*Me), 53.0 (C=N*C*H$_2$CH$_2$), 46.7 (CH$_2$*C*H$_2$NH$_2$), 46.1 (*C*H(Me)$_2$), 21.3 (CH(*C*H$_3$)$_2$), 10.8 (C(*C*H3) ppm.

Anal. Calcd. for ($C_{13}H_{26}N_4$) C: 65.50; H: 10.99; N: 23.50. Found: C: 65.67; H: 10.99; N: 23.36.

Synthesis and characterization of **[DPEN(Im^{iPr}H)NH$_2$][BF$_4$](5)** was performed according to literature procedure.[13]

Synthesis and characterization of [DPEN(Im^{iPr})NH$_2$] (6) by deprotonation of (5)

To a solution of 1.5 g (3.1 mmol; 1 eq) of **5** in 20 mL of THF was added 0.146 g (3.7 mmol; 1.2 eq) of $NaNH_2$. The reaction mixture was stirred for overnight at 40^{o}C. The solvent was removed *in vacuo* and the residue was extracted with three times 15 mL of pentane. The pentane was subsequently removed *in vacuo* to yield the product as a yellow oil (0.92 g, 2.4 mmol, 75%).

^{1}H NMR (300 MHz; $CDCl_3$): δ 7.18 – 6.90 (m, 10H, H_{Ar}), 4.70 (sept, 2H, J_{HH} 7.0 Hz, C*H*Me$_2$), 4.50 (d, 1H, J_{HH} 9.0 Hz, NH_2HC*H*(Ph)CH), 3.85 (d, 1H, J_{HH} 9.0 Hz, CNHC*H*(Ph)CH), 1.82 (s, 6H, CC*H*$_3$), 1.65 (bs, 2H, N*H*$_2$), 1.10 (d, 6H, J_{HH} 7.0 Hz, CH(CH_3)$_2$), 0.94 (d, 6H, J_{HH} 7.0 Hz, CH(CH_3)$_2$) ppm.

^{13}C NMR (100 MHz; $CDCl_3$): δ 154.1 (N_2C=N), 139.1 (*ipso*-C_{Ar}(CHNH$_2$)), 132.6 (*ipso*-C_{Ar}(CHN), 124.7 (C_{Ar}), 122.2 (C_{Ar}), 121.1 (C_{Ar}), 123.5 (*m*-C_{Ar}(CHNH$_2$)), 123.3 (*m*-C_{Ar}(CHNH), 123.0 (C_{Ar}), 118.2 (*C*Me) 70.3 (CNH*C*H(Ph)CH), 57.1 (NH_2H*C*H(Ph)CH), 46.2 (*C*HMe$_2$), 20.0 (CH(*C*H$_3$)$_2$), 19.5 (CH(*C*H$_3$)$_2$), 9.8 (C*C*H$_3$) ppm.

Anal. Calcd. for ($C_{25}H_{34}N_4$) C: 76.88; H: 8.77; N: 14.35. Found: C: 76.01; H: 8.98; N: 14.75.

Synthesis and characterization of the ligands BL^{iPr} **(7)**, DACH(Im^{iPr})$_2$ **(8)** were performed according to literature procedure.[13,31]

Preparation of the complexes

The complexes [Pd(en)Cl_2] and [Pd(BL^{iPr})Cl_2] are synthesized according to published procedure.[14,32]

Synthesis and characterization of [Pd(EAIm^{iPr})Cl$_2$] complex

To 111 mg (0.375 mmol; 1 eq) of [Pd(COD)Cl_2] was added 92.6 mg (0.35 mmol; 1 eq) of **4** in 10 mL of THF. The reaction mixture was stirred overnight at 55 ^{o}C affording an orange solution. The product was fully precipitated by the addition of 100 ml of n-hexane. The precipitate was filtered and dried *in vacuo*. The product was obtained as an orange-red solid (138.53 mg, 0.33 mmol, 89%).

^{1}H NMR (300 MHz; $CDCl_3$): δ = 5.40 (sept, 2H, J_{HH} 7.0 Hz, C$\underline{H}$(Me)$_2$), 4.13 (t, 2H, J_{HH} 4.9 Hz, C=NC$\underline{H}_2$CH$_2$), 2.68 (t, 2H, J_{HH} 5.0 Hz, CH$_2$C$\underline{H}_2$NH$_2$), 2.04 (s, 6H, CC$\underline{H}_3$), 1.60 (d, 6H, J_{HH} 7.0 Hz, CH(C$\underline{H}_3$)$_2$), 1.47 (d, 6H, J_{HH} 7.0 Hz, CH(C$\underline{H}_3$)$_2$)ppm.

^{13}C NMR (100 HMz; $CDCl_3$): δ = 152.7 (N$_2\underline{C}$=N), 118.6 ($\underline{C}$Me), 55.2 (C=N$\underline{C}$H$_2$CH$_2$), 48.6 (CH$_2\underline{C}$H$_2$NH$_2$), 47.4 ($\underline{C}$H(Me)$_2$), 22.4 (CH($\underline{C}$H$_3$)$_2$), 21.9 (CH($\underline{C}$H$_3$)$_2$), 10.9 (C($\underline{C}$H3) ppm.

Anal. Calcd. for ($C_{13}H_{26}Cl_2N_4Pd$) C: 37.56; H: 6.30; N: 13.48. Found: C: 36.99; H: 6.19; N: 13.33.

Synthesis and characterization of [Pd(DMEAIm^{iPr})Cl$_2$] complex

To 100 mg (0.338 mmol; 1 eq) of [Pd(COD)Cl_2] was added 95 mg (0.22 mmol; 1 eq) of **2** in 12 mL of THF. The reaction mixture was stirred overnight at the 40 °C affording a red precipitate. The precipitate was filtered and dried *in vacuo*. The product was obtained as a deep-red solid. Red crystals were obtained from CH_2Cl_2/n-hexane (139.42 mg, 0.32 mmol, 93%).

^{1}H NMR (300 MHz; $CDCl_3$): δ = 5.30 (sept, 2H, J_{HH} 7.0 Hz, C$\underline{H}$Me$_2$), 2.73 (t, 2H, J_{HH} 7.3 Hz, C=NC$\underline{H}_2$CH$_2$), 2.35 (t, 2H, J_{HH} 7.3 Hz, CH$_2$C$\underline{H}_2$NMe$_2$), 2.75 (s, 6H, N(C$\underline{H}_3$)$_2$), 2.05 (s, 6H, CC$\underline{H}_3$), 1.65 (d, 6H, J_{HH} 7.0 Hz, CH(C$\underline{H}_3$)$_2$), 1.52 (d, 6H, J_{HH} 7.0 Hz, CH(C$\underline{H}_3$)$_2$) ppm.

^{13}C NMR (100 MHz; $CDCl_3$): δ = 152.6 (N$_2\underline{C}$=N), 120.7 ($\underline{C}$Me), 68.2 (CH$_2\underline{C}$H$_2$NMe$_2$), 53.7 (C=N$\underline{C}$H$_2$CH$_2$), 51.3 (N($\underline{C}$H$_3$)$_2$), 48.8 ($\underline{C}$HMe$_2$), 22.7 (CH($\underline{C}$H$_3$)$_2$), 22.0 (CH($\underline{C}$H$_3$)$_2$), 10.09 (C$\underline{C}$H$_3$) ppm.

Anal. Calcd. for ($C_{15}H_{30}Cl_2N_4Pd$) C: 40.60; H: 6.81; N: 12.63. Found: C: 40.59; H: 6.78; N: 12.26.

Synthesis and characterization of [Pd(DPENIm^{iPr})Cl$_2$] complex

To 180 mg (0.608 mmol; 1 eq) of [Pd(COD)Cl_2] was added 250 mg (0.640 mmol; 1 eq) of **6** in 20 mL of THF. The reaction mixture was stirred for 8 h at room temperature, affording an orange solution. The complex was precipitated from solution by the addition of 100 ml of n-hexane. The precipitate was filtered and dried *in vacuo*. The product was obtained as an orange solid, the red crystals were obtained from aceton/n-hexane (363.3 mg, 0.91 mmol, 91%).

^{1}H NMR (300 MHz; $CDCl_3$): δ 7.38 – 7.10 (m, 10H, H$_{Ar}$), 5.31 (sept, 2H, J_{HH} 7.0 Hz, C$\underline{H}$Me$_2$), 4.98 (d, 1H, J_{HH} 9.0 Hz, NH$_2$HC$\underline{H}$(Ph)CH), 4.21 (d, 1H, J_{HH} 9.0 Hz, CNHC$\underline{H}$(Ph)CH), 2.04

(d, 3H, J_{HH} 7.0 Hz, CH(C<u>H</u>$_3$)$_2$), 1.99 (s, 6H, CC<u>*H*</u>$_3$), 1.85 (s, 2H, N<u>*H*</u>$_2$), 1.72 (d, 3H, J_{HH} 7.0 Hz, CH(C<u>H</u>$_3$)$_2$), 1.58 (d, 3H, J_{HH} 7.0 Hz, CH(C<u>H</u>$_3$)$_2$), 0.79 (d, 3H, J_{HH} 7.0 Hz, CH(C<u>H</u>$_3$)$_2$), ppm.

^{13}C NMR (100 MHz; $CDCl_3$): δ 156.2 (N$_2$<u>*C*</u>=N), 139.8 (*ipso*-<u>*C*</u>$_{Ar}$(CHNH$_2$)), 132.9 (*ipso*-<u>C</u>$_{Ar}$(CHN), 125.1 (<u>*C*</u>$_{Ar}$), 122.9 (<u>*C*</u>$_{Ar}$), 121.8 (<u>*C*</u>$_{Ar}$), 124.2 (*m*-<u>*C*</u>$_{Ar}$(CHNH$_2$)), 123.9 (*m*-<u>*C*</u>$_{Ar}$(CHNH), 123.5 (<u>*C*</u>$_{Ar}$), 119.5 (<u>*C*</u>Me) 72.1 (CNH<u>*C*</u>H(Ph)CH), 59.3 (NH$_2$H<u>*C*</u>H(Ph)CH), 48.4 (<u>*C*</u>HMe$_2$), 47.2 (<u>*C*</u>HMe$_2$), 22.2 (CH(<u>*C*</u>H$_3$)$_2$), 21.5 (CH(<u>*C*</u>H$_3$)$_2$), 21.0 (CH(<u>*C*</u>H$_3$)$_2$), 20.6 (CH(<u>*C*</u>H$_3$)$_2$), 10.8 (C<u>*C*</u>H$_3$), 10.5 (C<u>*C*</u>H$_3$) ppm.

Anal. Calcd. for ($C_{25}H_{34}Cl_2N_4Pd$) C: 52.87; H: 6.03; N: 9.87. Found: C: 52.97; H: 6.14; N: 10.01.

Synthesis and characterization of [Pd(DACH(Im^{iPr})$_2$)Cl$_2$] complex

To 100 mg (0.340 mmol; 1 eq) of [Pd(COD)Cl_2] was added 113.2 mg (0.240 mmol; 1 eq) of **6** in 20 mL of THF. The reaction mixture was stirred during 30 min at 50 ^{O}C and then stirred at room temperature during the night, affording a red solution. The complex was precipitated from solution by the addition of 100 ml of n-hexane. The precipitate was filtered and dried *in vacuo*. The product was obtained as a red solid (186.1 mg, 0.29 mmol, 85%).

^{1}H NMR (300 MHz; $CDCl_3$): δ = 5.45 (sept, 2H, C<u>*H*</u>Me$_2$), 5.28 (sept, 2H, C<u>*H*</u>Me$_2$), 3.82 (bs, 4H, CH$_2$C<u>*H*</u>(N=C)C<u>*H*</u>(N=C)CH$_2$), 2.72 - 2.60 (m, 2H, C<u>*H*</u>$_2$), 2.15 (s, 6H, CC<u>*H*</u>$_3$), 2.05 (s, 6H, CC<u>*H*</u>$_3$) 2.10 - 1.92 (m, 2H, C<u>*H*</u>$_2$), 1.89 -1.81 (m, 2H, C<u>*H*</u>$_2$), 1.78 - 1.69 (m, 2H, C<u>*H*</u>$_2$), 1.62 (d, 6H, J_{HH} 7.0 Hz, CH(C<u>*H*</u>$_3$)$_2$), 1.52 (d, 6H, J_{HH} 7.0 Hz, CH(C<u>*H*</u>$_3$)$_2$), 1.43 (d, 6H, J_{HH} 7.0 Hz, CH(C<u>*H*</u>$_3$)$_2$), 1.08 (d, 6H, J_{HH} 7.0 Hz, CH(C<u>*H*</u>$_3$)$_2$) ppm.

^{13}C NMR (100 MHz; $CDCl_3$): δ = 153. (N$_2$<u>*C*</u>=N), 117.8 (<u>*C*</u>Me), 65.7 (CH$_2$<u>*C*</u>H(N=C)<u>*C*</u>H(N=C)CH$_2$), 50.1 (<u>*C*</u>HMe$_2$), 49.3 (<u>*C*</u>HMe$_2$), 36.9 (<u>*C*</u>H$_2$), 26.5 (<u>*C*</u>H$_2$), 23.7 (CH(<u>*C*</u>H$_3$)$_2$), 22.5 (CH(<u>*C*</u>H$_3$)$_2$), 21.6 (CH(<u>*C*</u>H$_3$)$_2$), 21.0 (CH(<u>*C*</u>H$_3$)$_2$), 13.1 (C<u>*C*</u>H$_3$), 12.3 (C<u>*C*</u>H$_3$) ppm.

Anal. Calcd. for ($C_{28}H_{50}Cl_2N_6Pd$) C: 51.89; H: 7.78; N: 12.97. Found: C: 51.26; H: 7.93; N: 12.01.

ESI-HRMS: [M-Cl]$^+$: Calcd.: 611.28; Found: 611.14 (Δ: 0.41 mmu).

Preparation of aqua complexes

The aqua complexes of Pd(II) complexes were prepared starting from the corresponding chlorido complexes. The conversion was performed by the addition of the corresponding amount of $AgClO_4$ to a solution of the chloride complex and stirring for 5 h at 50 °C. The white precipitate that formed (AgCl) was filtered off using a Millipore filtration unit, and the solutions were diluted. Great care was taken to ensure that the resulting solution was free of Ag^+ ions and that the chlorido complexes had been completely converted into the aqua form. Since it is well known that perchlorate ions do not coordinate to Pd(II) and Pt(II) in aqueous solution,[33] pH titrations were studied in perchlorate medium.

Instrumentation and measurements

NMR spectra were recorded on Bruker DPX 200, DRX 400 and AV 300 devices. Chemicals shifts (δ) are reported in ppm and referenced to tetramethylsilane (1H, ^{13}C) and trichlorofluoromethane (^{19}F). Coupling constants (*J*) are reported in Hertz (Hz) and splitting patterns are indicated as s (singlet), d (doublet), t (triplet), sept (septet), bs (broad signal) and m (multiplet). Elemental analyses (C, H, N) were performed by combustion and gas chromatographic analysis with an Elementar Vario MICRO elemental analyzer. High resolution electron spray ionization (ESI) mass spectroscopy was performed on a Finnigan MAT 95 XL Trap device. pH measurements were carried out using a Mettler Delta 350 digital pH meter with a resolution ± 0.01 mV, with a combination glass electrode. This electrode was calibrated using standard buffer solutions of pH 4, 7 and 9 obtained from Sigma. Kinetic measurements of the Pd(II) complex were carried out on an Applied Photophysics SX.18MV stopped-flow instrument coupled to an on-line data acquisition system. The temperature was controlled throughout all kinetic experiments to ± 0.1°C. All kinetic measurements were performed under *pseudo*-first-order conditions, *i.e.*, at least a 10-fold excess of the nucleophile was used. Uv-Vis spectra were recorded on PerkinElmer Lamda 35 double-beam spectrophotometer equipped with thermostated 1.00-cm quartz Suprasil cells.

Determination of the p*K*a value of the Pd(II) complexes

Spectrophotometric pH titrations of the solutions of the complexes were performed with NaOH as a base at 298 K. To avoid absorbance corrections due to dilution, a large volume (300

mL) of the complex solution was used in the titration. The change in pH from 2 to approximately 3 was achieved by addition of known amounts of crushed pellets of NaOH. The consecutive pH changes were obtained by adding drops of saturated solutions of NaOH, 1 or 0.1 M, using a micropipette. To avoid contamination released by the pH electrode, it was necessary to take 2-mL aliquots from the solution into narrow vials for the pH measurements. The aliquots were discarded after the measurements. The total reversibility of the titration could be achieved by subsequent addition of $HClO_4$.

The titration data for the complexes were fitted to the following Eq. (5) for the determination of both pK_a values[34-36] and the obtained data are presented in Table 2.

$$y = a + (b - a)/(1 + 2.718*((x - pK_{a1}/m)) + (c - b)/(1 + 2.718*((x - pK_{a2})/n)) \quad (5)$$

The parameter a represents the value of the absorbance at the beginning of the titration, b represents the absorbance during the titration and c is the absorbance at the end of the titration. The parameters m and n are used to optimize the titration curve. In this equation y represents absorbance value and x refers to the pH.

Solubility measurements

The concentrations of saturated solutions of the studied Pd(II) complexes were determined by UV-vis spectrophotometry. Therefore the specific absorptivity of the compounds in the water was determined first. This was measured using five dilution series (5, 10, 30, 40, 50 mM) of the studied complexes, then the calibration curve was calculated using Lambert-Beer law. The slope of the curve gave specific absorptivity.

The required quantity of water solution was added to the 5 ml volumetric flask. The solution was heated up to 298 K. Previously weighed quantity of Pd(II) complexes was added to the volumetric flask until the saturation point occurs. Stirring was continued up to 7 hours at 298 K. The sample was filtered through 0.20 μm membrane filter. A measured quantity of filtered sample was transferred into another volumetric flask and made further dilutions. The absorbance was measured using UV-vis spectrophotometry. The same process was repeated two times.

Kinetic Measurements

The substitution reactions of the Pd(II) complex with the nucleophiles: TU, L-Met, L-His and Gly were studied spectrophotometrically by following the change in absorbance at suitable wavelengths as a function of time. Spectral changes resulting from the mixing of the complex and nucleophile solutions were recorded over the wavelength range 200 to 400 nm to establish a suitable wavelength at which kinetic measurements could be performed.

Substitution reactions were initiated by mixing equal volumes of complex and ligand solutions directly in the stopped-flow instrument and followed for at least eight half-lives. The substitution process was monitored as a change in absorbance with time under *pseudo*-first-order conditions. The observed *pseudo*-first-order rate constants, k_{obsd}, were calculated as the average value from four to six independent kinetic runs using the program OriginPro 8. Experimental data are reported in Tables S3-S26 (Supporting information).

X-ray diffraction studies

Data were recorded at 100(2) K using an Oxford Diffraction Nova A diffractometer with monochromated Cu *K*α radiation. The structures were refined anisotropically using the SHELXL-97 program.[37] Hydrogen atoms were either (i) located and refined isotropically (NH_2), (ii) included as idealized methyl groups allowed to rotate but not tip or (iii) placed geometrically and allowed to ride on their attached carbon atoms. *Special features*: **[Pd(DMEAIm^{iPr})Cl$_2$]•2CH$_2$Cl$_2$** crystallizes as half a molecule on a crystallographic mirror plane perpendicular to the five-membered ring. The ethylene bridge is disordered across the mirror plane. The structure of **[Pd(DPENIm^{iPr})Cl$_2$] •5/4 C$_3$H$_6$O • 1/4 C$_6$H$_{14}$** contains four ordered molecules of acetone, one disordered molecules of acetone and one disordered molecule of hexane in the asymmetric unit. The latter two were removed mathematically with the program SQUEEZE.[38] Derived parameters such as the formular weight correspond to four additional molecules of aceton and four molecules of hexane per cell.

	[Pd(DMEAIm^{iPr})Cl$_2$]•2CH$_2$Cl$_2$	**[Pd(DPENIm^{iPr})Cl$_2$] •5/4 C$_3$H$_6$O • 1/4 C$_6$H$_{14}$**
Empirical Formula	$C_{17}H_{34}Cl_6N_4Pd$	$C_{30.25}H_{45}Cl_2N_4O_{1.25}Pd$
Formula Weight	613.58	662.00
Crystal System	orthorhombic	orthorhombic
Space Group	*P*nma	$P2_12_12_1$
a/Å	16.5015(4)	14.8839(3)
b/Å	19.3631(5)	28.4936(9)
c/Å	8.2474(2)	30.6466(9)
Volume [Å^3]	2635.21(11)	12997.1(6)
Z	4	16
Reflections Collected	25762	158785
Independent reflections	2857 [R_{int} = 0.0391]	26899 [R_{int} = 0.0654]
ρ_C/g cm^{-3}	1.547	1.345
μ/mm^{-1}	11.366	6.331
$R(F_O)$, [$I > 2\sigma(I)$]	0.0246	0.0376
Rw (F_O^2)	0.0612	0.0890
Goodness of fit on (F^2)	1.071	1.052
Flack parameter	–	0.005(4)
$\Delta\rho$/eÅ^{-3}	0.450/–0.806	0.895/–1.145

References:

1. Ž. D. Bugarčić, J. Bogojeski and R. van Eldik, *Coord. Chem. Rev.,* 2015, **292**, 91.
2. B. Lippert (ed.), *Cisplatin, Chemistry and Biochemistry of Leading Antitumor Drugs*, Wiley-VCH, Zürich, 1999; D. Wang and S. J. Lippard, *Nat. Rev. Drug Discovery*, 2005, **4**, 307; S. van Zutphen and J. Reedijk, *Coord. Chem. Rev*., 2005, **24**, 2845; H. Zorbas and B. K. Keppler, *ChemBioChem*, 2005, **6**, 1157.
3. E. Alessio (ed.), *Bioinorganic Medicinal Chemistry*, Wiley-VCH, Weinheim, 2011, Chapters 1–4.
4. P. E. N. Barry and J. P. Sadler, *Chem. Commun.,* 2013, **49**, 5106.
5. L. Ronconi and J. P. Sadler, *Coord. Chem. Rev.,* 2007*,* **251**,1633.
6. B. Rosenberg, L. V. Camp, J. E. Trosko and V. H. Mansour, *Nature*, 1969, **222**, 385.
7. A. S Abu-Surrah and M. Kettunen, *Curr. Med. Chem.*, 2006, **13***,* 1337.
8. E. Gao , C. Liu , M. Zhu , H. Lin , Q. Wu and L. Liu , *Anticancer Agents Med Chem*., 2009, **9**, 356.
9. E. Gao, M. Zhu, H. Yin, L. Liu, Q. Wu and Y. Sun, *J. Inorg. Biochem*., 2008, **102**, 1958.
10. X. Wu and M. Tamm, *Coord. Chem. Rev.,*2014, **260**, 116.
11. T. Glöge, D. Petrović, C. G. Hrib, C. Daniliuc, E. Herdtweck, P. G. Jones and M. Tamm, *Z. Anorg. Allg. Chem.*, 2010, **636**, 2303.
12. T.K. Panda, S. Randoll, C.G. Hrib, P.G. Jones, T. Bannenberg and M. Tamm, *Chem.Commun*., 2007, 5007; T.K. Panda, D. Petrovic, T. Bannenberg, C.G. Hrib, P.G. Jones and M. Tamm, *Inorg. Chim. Acta*, 2008, **361**, 2236; T.K. Panda, A.G. Trambitas, T. Bannenberg, C.G. Hrib, S. Randoll, P.G. Jones and M. Tamm, *Inorg. Chem.,* 2009, **48**, 5462; A.G. Trambitas, T. K. Panda, J. Jenter, P. Roesky, C.G. Daniliuc, C.G. Hrib, P.G. Jones and M. Tamm, *Inorg. Chem*., 2010, **49**, 2435; T.K. Panda, C.G. Hrib, P.G. Jones and M. Tamm, *J. Organomet. Chem*., 2010, **695**, 2768; M. Tamm, A.G. Trambitas, C.G. Hrib and P.G. Jones, *Terrae Rarae*, 2010, **7**, 1; A.G. Trambitas, J. Yang, D. Melcher, C.G. Daniliuc, P.G. Jones, Z. Xie and M. Tamm, *Organometallics*, 2011, **30**, 1122; A.G. Trambitas, D. Melcher, L. Hartenstein, P.W. Roesky, C. Daniliuc, P.G.Jones and M. Tamm, *Inorg. Chem*., 2012, **51**, 6753.
13. J. Volbeda, P. G. Jones and M. Tamm*, Inorg. Chim. Acta,* 2014, **422**, 158.

14. J. Bogojeski, R. Jelić, D. Petrović, E. Herdtweck, P. G. Jones, M. Tamm and Ž. D. Bugarčić, *Dalton Trans*., 2011, **40**, 6515.
15. (a) J. Börner, U. Flörke, K. Huber, A. Döring, D. Kuckling, S. Herres-Pawlis, *Chem. Eur. J*., 2009, **15**, 2362-2376; V. Raab, K. Harms, J. Sundermeyer, B. Kovačević, Z.B. Maksić, J. Org. Chem., 2003, **68**, 8790-8797;(c) A. Neuba, R. Haase, M. Bernard, U. Flörke, S. Herres-Pawlis, Z. Anorg. Allg. Chem., 2008, **634**, 2511-2517.
16. R. C. Boyle, J. T. Mague, M. J. Fink, *Acta Cryst.*, 2004, **E60**, m40-m41.
17. Ž. D. Bugarčić, J. Bogojeski, B. Petrović, S. Hochreuther and R. van Eldik , *Dalton Trans.*, 2012, **41,** 12329-12345.
18. T. Rau, R. van Eldik, *Interactions of metal ions with nucleotides, nucleic acids, and their constituents,* in: Sigel, A., Sigel, H. (Eds.), *Metal Ions in Biological Systems*, Marcel Dekker, New York, 1996, 339.
19. S.J. Barton, K.J. Barnham, A. Habtemariam, R.E. Sue and R.J. Sadler, *Inorg. Chim. Acta*, 1998, **273**, 8.
20. Y. Xu, J. Cui and D. Puett, *Cancer Bioinformatics*, Springer, 2014, p. 209.
21. M. T. Ashby, *Comments Inorg. Chem.* 1990, **10**, 297.
22. S. G. Murray and F. R. Hartley, *Chem. Rev.* 1981, **81**, 365.
23. J. Reedijk, *J. Chem. Commun.* 1996, 801.
24. J. H. Burchenal, K. Kalaher, K. Dew, L. Lokys and G. Gale, *Biochimie*, 1978, **60**, 961.
25. M. L. Tobe and J. Burgess (eds.) *Inorganic Reaction Mechanism,* Longman, England, 1999, p. 70, p. 364
26. N. Summa, W. Schiessl, R. Puchta, N. van Eikema Hommes and R. van Eldik, *Inorg. Chem.*, 2006, **45**, 2948.
27. E. J. Cohn and J. T. Edsall (eds.) *Proteins, Amino Acids and Peptides as Ions and Dipolar Ions*, Reinhold Publishing Corporation, New York, 1943.
28. N. Summa, T. Soldatović, L. Dahlenburg, Ž. D. Bugarčić and R. van Eldik, *J Biol Inorg Chem*, 2007, **12**, 461.
29. B. Petrović, Ž. D. Bugarčić and R. van Eldik, *Dalton Trans.*, 2008, 807.
30. R. A. Kunetskiy, S. M. Polyakova, J. Vavrík, I. Císarová, J. Saame, E. R. Nerut, I. Koppel, I. A. Koppel, A. Kütt, I. Leito and I. M. Lyapkalo, *Chem. Eur. J.,* 2012, **18**, 3621.

31. D. Petrović, T. Bannenberg, S. Randoll, P. G. Jones and M. Tamm, *Dalton Trans.*, 2007, 2812;
32. H. Hohmann and R. van Eldik, *Inorg. Chim. Acta,* 1990, **174**, 87.
33. T. G. Appleton, J. R. Hall, S. F. Ralph and C. S. M. Thompson, *Inorg. Chem.,* 1984, **23**, 3521.
34. T. Soldatović, S. Jovanović, Ž.D. Bugarčić and R. van Eldik, *Dalton Trans.*, 2012, **41**, 876.
35. A. Mambanda, D. Jaganyi, S. Hochreutther and R. van Eldik, *Dalton Trans.*, 2010, **39**, 3595.
36. (*a*) A. Hofmann and R. van Eldik, *Dalton Trans.*, 2003, 2979; (*b*) H.Erturk, A. Hofmann, R. Puchta and R. van Eldik, *Dalton Trans.*, 2007, 2295; (*c*) H. Erturk, J. Maigut, R. Puchta and R. van Eldik, *Dalton Trans.*, 2008, 2759; (*d*) H. Erturk, R. Puchta and R. van Eldik, *Eur. J. Inorg. Chem.*, 2009, 1334.
37. G. M. Sheldrick, SHELXL-97, Program for the Refinement of Crystal Structure from Diffraction Data, University of Göttingen, Göttingen, Germany, 1997.
38. Part of the PLATON suite; A. Spek, University of Utrecht, Netherlands, 2009.

Table 1. The water solubility of imidazolin-2-imine Pd(II) complexes at 298 K.

Complex	Solubility in water at 298 K mg/ml
$[Pd(EAIm^{iPr})(H_2O)_2]^{2+}$	10.5
$[Pd(DMEAIm^{iPr})(H_2O)_2]^{2+}$	10.2
$[Pd(DPENIm^{iPr})(H_2O)_2]^{2+}$	10.1
$[Pd(BL^{iPr})(H_2O)_2]^{2+}$	9.5
$[Pd(DACH(Im^{iPr})_2)(H_2O)_2]^{2+}$	8.5
Cisplatin[A]	2.5
Oxaliplatin[B]	5.0

[A] The Merck Index, 12th ed., Entry# 2378
[B] According to Sigma-Aldrich

Table 2. Summary of p*K*a values obtained for the stepwise deprotonation of the coordinated water ligands in Pd(II) complexes

	p*K*a$_1$	**p*K*a$_2$**
$[Pd(en)(H_2O)_2]^{2+}$,[18]	5.60 ± 0.05	7.30 ± 0.05
$[Pd(EAIm^{iPr})(H_2O)_2]^{2+}$	5.45 ± 0.10	7.62 ± 0.20
$[Pd(DMEAIm^{iPr})(H_2O)_2]^{2+}$	5.75 ± 0.10	8.28 ± 0.10
$[Pd(DPENIm^{iPr})(H_2O)_2]^{2+}$	7.17 ± 0.20	11.21 ± 0.10
$[Pd(BL^{iPr})(H_2O)_2]^{2+}$,[14]	6.18 ± 0.05	10.07 ± 0.05
$[Pd(DACH(Im^{iPr})_2)(H_2O)_2]^{2+}$	7.56 ± 0.20	8.39 ± 0.20

Table 3. The rate constants for the first reaction step of the substitution reactions of the Pd(II) complexes with TU, L-Met, Gly and L-His at pH = 7.2 (25 mM Hepes buffer) in the presence of 30 mM NaCl at 310 K.

first reaction step	**TU** $k_1[M^{-1} s^{-1}]$	**L-Met** $k_1[M^{-1} s^{-1}]$	**Gly** $k_1[M^{-1} s^{-1}]$	**L-His** $k_1[M^{-1} s^{-1}]$
$[Pd(en)Cl_2]$	$(6.95 \pm 0.10)\ 10^5$	$(5.05 \pm 0.10)\ 10^5$	$(1.02 \pm 0.10)\ 10^4$	$(2.87 \pm 0.20)\ 10^5$
$[Pd(EAIm^{iPr})Cl_2]$	$(1.25 \pm 0.20)\ 10^5$	$(5.54 \pm 0.20)\ 10^4$	$(1.45 \pm 0.10)\ 10^3$	$(2.78 \pm 0.10)\ 10^3$
$[Pd(DMEAIm^{iPr})Cl_2]$	$(6.78 \pm 0.20)\ 10^3$	$(4.5 \pm 0.10)\ 10^3$	$(1.28 \pm 0.10)\ 10^3$	$(2.00 \pm 0.20)\ 10^3$
$[Pd(DPENIm^{iPr})Cl_2]$	$(5.13 \pm 0.20)\ 10^3$	$(2.53 \pm 0.20)\ 10^3$	$(8.52 \pm 0.20)\ 10^2$	$(1.48 \pm 0.20)\ 10^3$
$[Pd(BL^{iPr})Cl_2]$	$(9.20 \pm 0.20)\ 10^2$	$(5.15 \pm 0.20)\ 10^2$	$(2.93 \pm 0.20)\ 10^2$	$(1.67 \pm 0.20)\ 10^2$
$[Pd(DACH(Im^{iPr})_2)Cl_2]$	$(1.64 \pm 0.20)\ 10^2$	$(1.51 \pm 0.20)\ 10^2$	97.70 ± 0.10	$(1.35 \pm 0.10)\ 10^2$

Table 4. The rate constants for the second reaction step of the substitution reactions of the Pd(II) complexes with TU, L-Met, Gly and L-His at pH = 7.2 (25 mM Hepes buffer) in the presence of 30 mM NaCl at 310 K.

second reaction step	**TU** $k_2[M^{-1} s^{-1}]$	**L-His** $k_2[M^{-1} s^{-1}]$
$[Pd(en)Cl_2]$	$(1.53 \pm 0.20)\ 10^4$	$(1.03 \pm 0.10)\ 10^4$
$[Pd(EAIm^{iPr})Cl_2]$	$(8.52 \pm 0.10)\ 10^2$	70.20 ± 0.10
$[Pd(DMEAIm^{iPr})Cl_2]$	$(4.22 \pm 0.10)\ 10^2$	43.80 ± 0.10
$[Pd(DPENIm^{iPr})Cl_2]$	$(2.80 \pm 0.20)\ 10^2$	39.20 ± 0.20
$[Pd(BL^{iPr})Cl_2]$	$(1.84 \pm 0.10)\ 10^2$	24.30 ± 0.10
$[Pd(DACH(Im^{iPr})_2)Cl_2]$	70.90 ± 0.10	19.20 ± 0.10

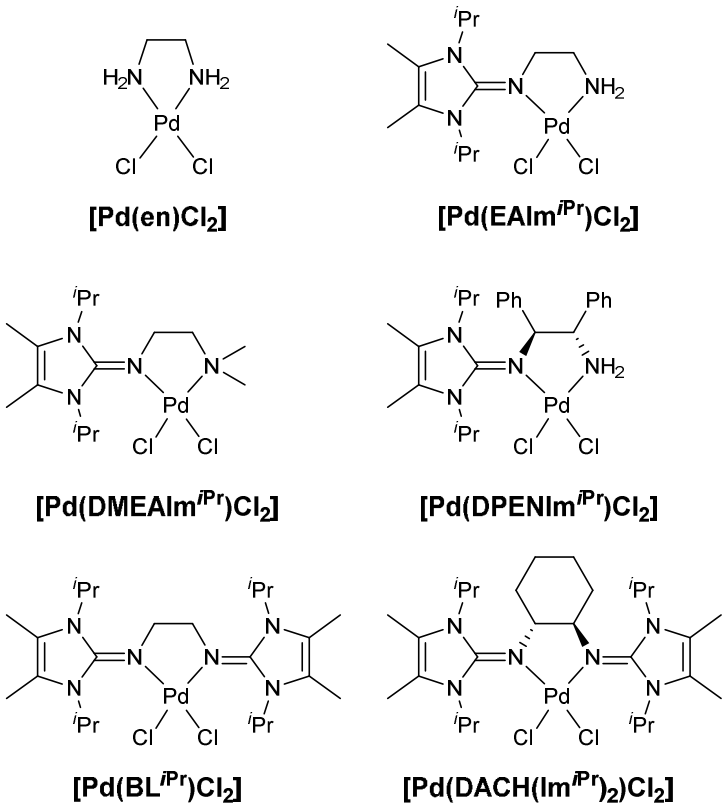

Figure 1. Structures of the investigated Pd(II) complexes, along with their abbreviations.

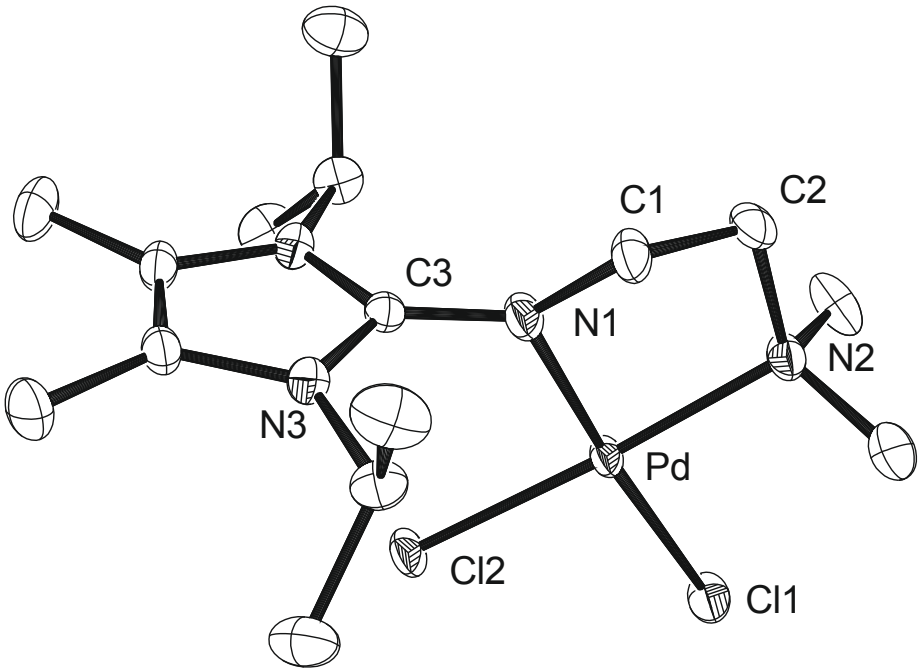

Figure 2. ORTEP drawing of [Pd(DMEAIm$^{i\text{Pr}}$)Cl_2]·CH_2Cl_2 with thermal displacement parameters drawn at 50% probability. The alternative disordered positions of C1 and C2, hydrogen atoms and a co-crystallized molecule of CH_2Cl_2 were omitted for clarity. Selected bond distances [Å] and angles [°]: Pd-N1 2.013(2), Pd-N2 2.076(2), Pd-Cl1 2.3390(7), Pd-Cl2 2.2951(7), N1-C3 1.349(4), N3-C3 1.352(2); N1-Pd-N2 83.08(9), Cl1-Pd-Cl2 92.91(7).

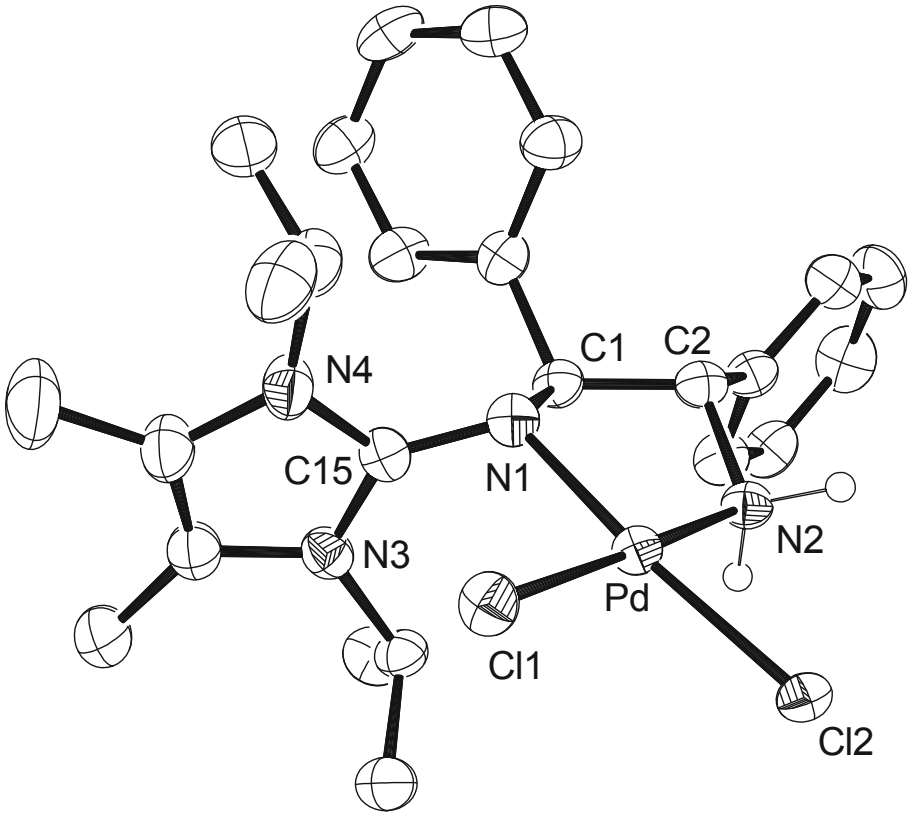

Figure 3. ORTEP drawing of one of the four molecules of [Pd(DPENImiPr)Cl_2] in [Pd(DPENImiPr)Cl_2]·acetone with thermal displacement parameters drawn at 50% probability. Hydrogen atoms and a co-crystallized molecule of acetone were omitted for clarity. Selected bond distances [Å] and angles [°]: Pd-N1 2.034(4), Pd-N2 2.038(3), Pd-Cl1 2.3193(10), Pd-Cl2 2.3395(10), N1-C15 1.367(5), N3-C15 1.363(5) N4-C15 1.359(6); N1-Pd-N2 82.69(14), Cl1-Pd-Cl2 91.85(4).

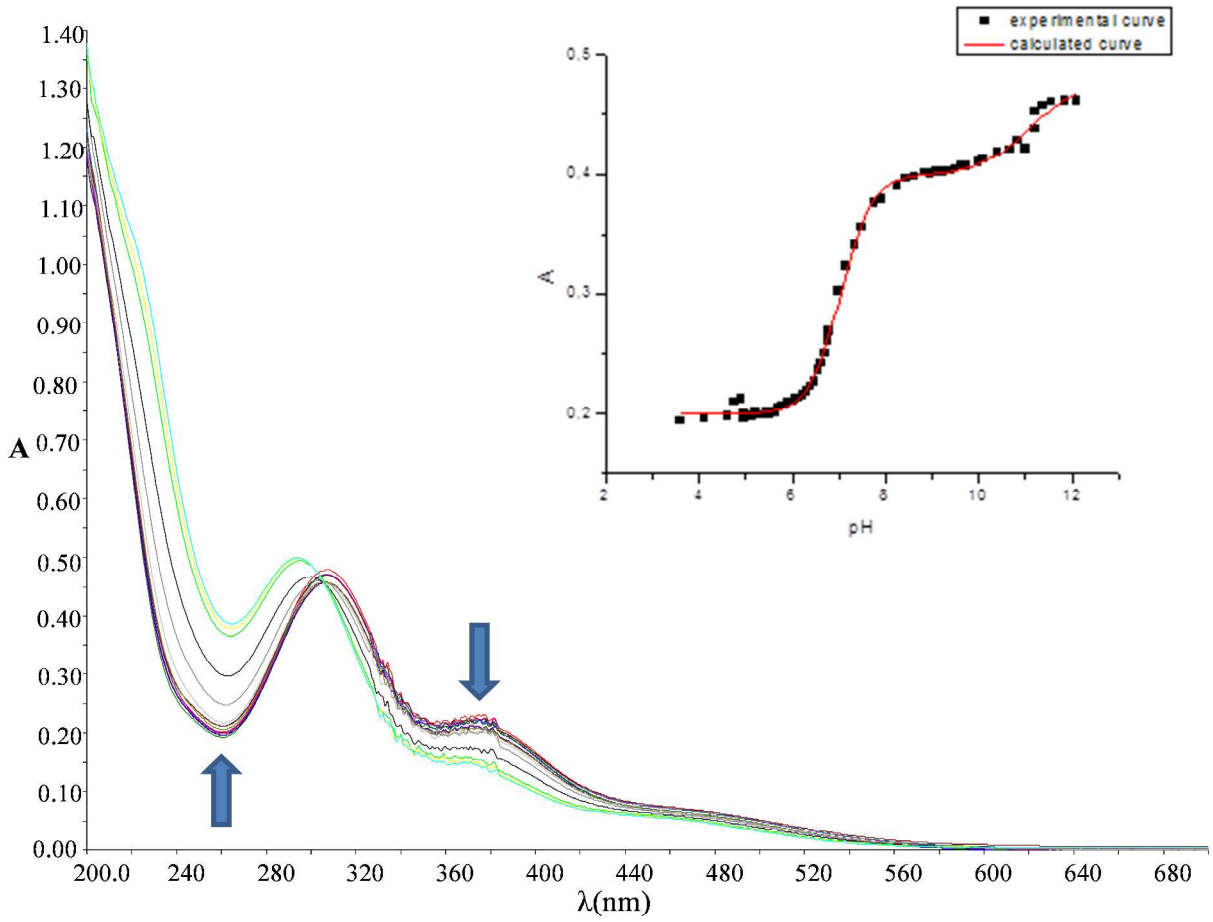

Figure 4. UV-vis spectra recorded for 0.1 mM $[Pd(DPENIm^{iPr})(H_2O)_2]^{2+}$ in the pH range 2 to 12 at 25 °C. Insert: Plot of absorbance *vs* pH at 260 nm (experimental curve and calculated curve).

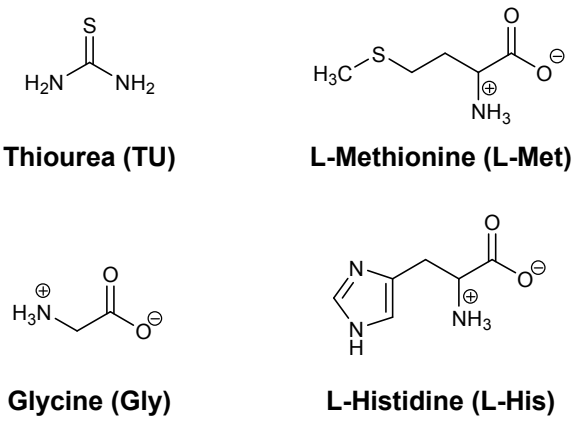

Figure 5. Structures of the investigated nucleophiles, along with the used abbreviations.

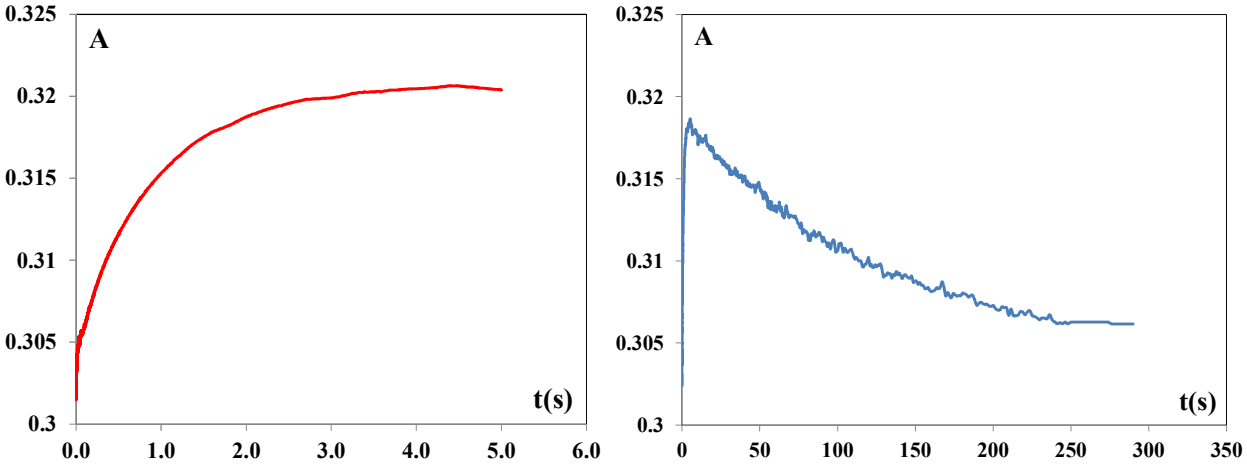

Figure 6. Absorbance-time traces for the reaction between [Pd(DMEAIm^{iPr})Cl$_2$] and TU ($2 \cdot 10^{-4}$ M), the left graph presents an absorbance-time traces for the first substitution step, the right graph presents an absorbance-time traces for both substitution steps at pH 7.2, 310 K in 25 mM Hepes buffer and 30 mM NaCl.

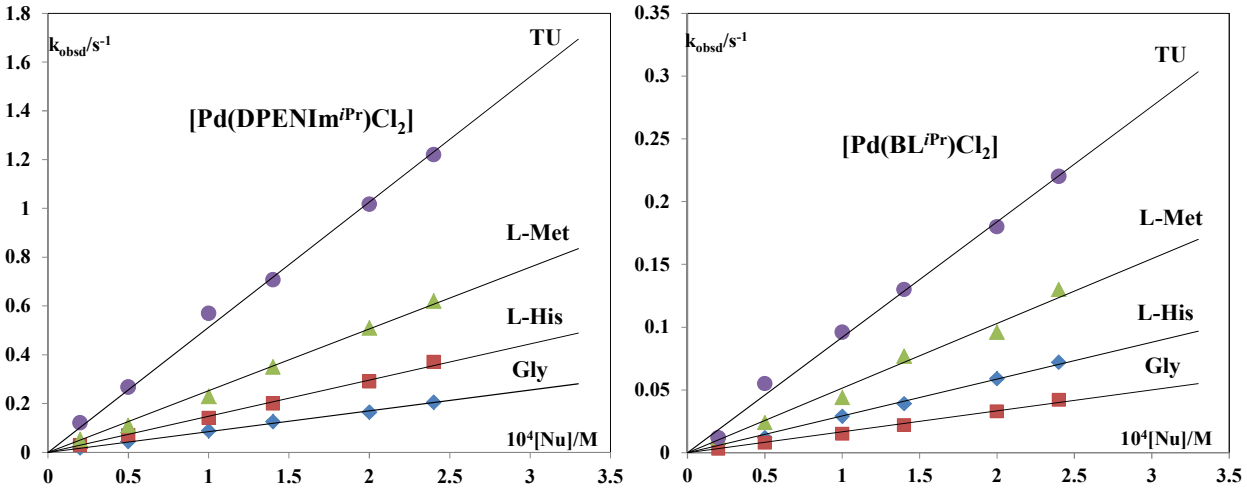

Figure 7. *Pseudo*-first-order rate constants plotted as a function of nucleophile concentration for the first step of the substitution reactions of the [Pd(DPENIm^{iPr})Cl$_2$] and [Pd(BL^{iPr})Cl$_2$] complexes with TU, L-Met, L-His and Gly at pH = 7.2 and 310 K in 25 mM Hepes buffer and 30 mM NaCl.

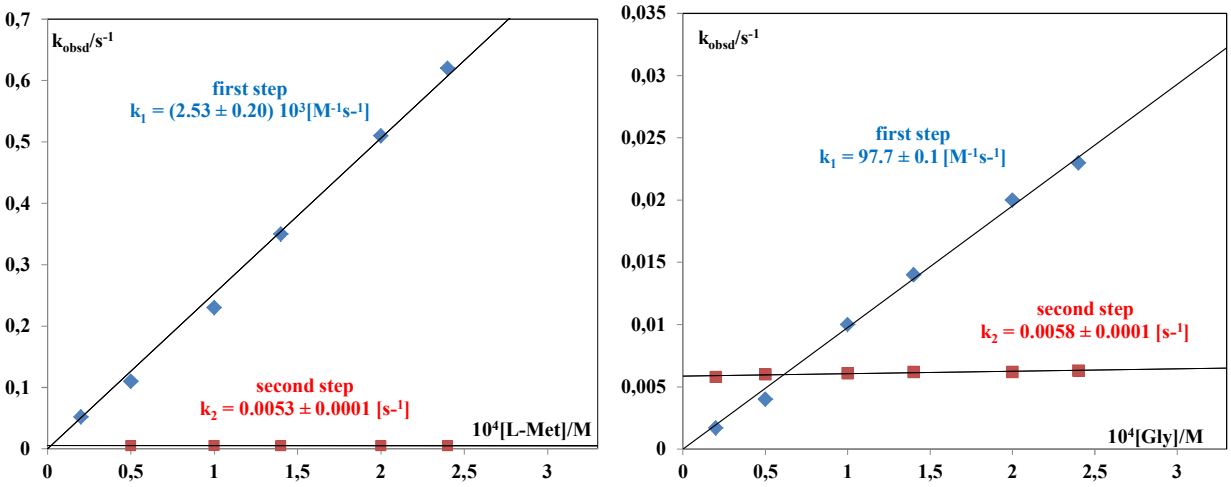

Figure 8. Plots of k_{obsd} versus L-Met concentration for the [Pd(DPENIm$^{i\text{Pr}}$)Cl$_2$] complex and plots of k_{obsd} versus Gly concentration for the [Pd(DACH(Im$^{i\text{Pr}}$)$_2$)Cl$_2$] complex (pH = 7.2, 310 K, 25 mM Hepes buffer, 30 mM NaCl)

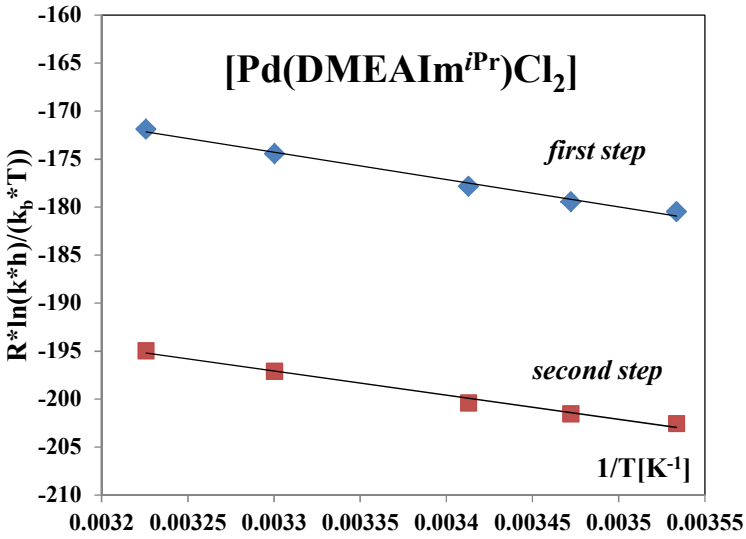

Figure 9. Eyring plots for the two reaction steps of [Pd(DMEAIm^{iPr})Cl$_2$] complex with TU at pH = 7.2, 310 K, 25 mM Hepes buffer, 30 mM NaCl